

## Structure and Kinetics of Cluster Decomposition of Polystyrene Star Chains in Dilute Solutions

Hong Huo, Fan Jin, and To Ngai\*

Department of Chemistry, The Chinese University of Hong Kong, Shatin, N.T., Hong Kong

Received June 12, 2007

Revised Manuscript Received August 2, 2007

During the past two decades, many studies, both theoretical and experimental, have been devoted to the formation and structure of polymer clusters by association or cross-linking polymer chains in solution.<sup>1–3</sup> Conceptually, one starts with a dispersion of monodispersed polymer chain. Upon clustering, these chains collide due to their Brownian motion and stick together irreversibly to form clusters. These clusters themselves continue to diffuse, collide, and form hyperbranched clusters. Although the reasons for clustering are complex and vary from one system to another due to the different physical or chemical origins, there have been significant advances in our understanding of such a cluster–cluster “aggregation” process in recent years. The key to these advances is the recognition that the formed clusters have fractal structures, allowing a more detailed study of the aggregation process and the relationship of cluster structures to the aggregation kinetics.<sup>4</sup>

It is well-known that two distinct, limiting regimes of aggregation have been identified in the classical colloidal sciences.<sup>5,6</sup> Depending on the sticking probability ( $P_s$ ) between two colloidal particles, they correspond directly to the diffusion-limited cluster–cluster aggregation (DLCA,  $P_s \sim 100\%$ ) and the reaction-limited cluster–cluster aggregation (RLCA,  $P_s \ll 100\%$ ).<sup>7–9</sup> Both aggregation processes are found to have characteristic, yet distinct, features. The structures of the formed cluster in both regimes can be quantitatively characterized by scaling behavior, namely, the mass ( $M$ ) of the clusters scales to the size ( $R$ ) with different fractal dimensions ( $d_f$ ) as  $M \propto R^{d_f}$ . The fractal dimension is  $d_f \approx 1.7–1.8$  for DLCA and  $d_f \approx 2.1–2.5$  for RLCA because DLCA leads to a more open and less uniform structure. Nonetheless, RLCA can result in a compact aggregate. For the aggregation kinetics for DLCA,  $R$  is characterized by  $R \propto t^\gamma$  with  $\gamma < 1$  and typically  $\gamma = 1/d_f$ , whereas for RLCA,  $R \propto e^{t/\tau_R}$ , where  $\tau_R$  is a constant, depending on the dispersion nature.<sup>8,9</sup> It is helpful to note that both theory and experiment have indicated that other processes, which can be described as crossovers between DLCA and RLCA, exist.<sup>10,11</sup> Moreover, the formation of more compact structures (with  $d_f > 2.5$ ) than expected for RLCA processes has been encountered and explained in terms of cluster restructuring or reaction reversibility.<sup>12–14</sup> In this case, the sticking between subunits is considered to be reversible so that they can loosen and re-form repeatedly after collision.

Practically, the study of the cluster structures and aggregation kinetics requires considerable experimental care. Faster aggregation rate leads to the DLCA process but also possibly follows into the intermediate regime; while for RLCA, the aggregation rate should be slow in order to have sufficient time to collect the data without a change in the cluster structure and size. Ideally, we need a system in which the clustering process can be stopped at each desired stage so that we can study the

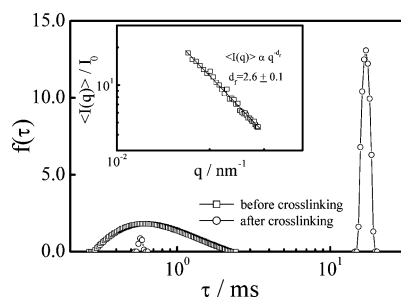
clusters formed inside and then let it proceed again. On the other hand, if not impossible, we need a system that the formed clusters can be decomposed (fragmented). In this way, we are able to tune the system back to a certain extent and study the structures of fragments as well as the decomposition kinetics. Experimentally, the decomposition of polymer clusters or gel networks has not attracted much sufficient attention, principally due to the difficulty in finding a proper system.<sup>15</sup>

Recently, we have used atom transfer radical polymerization (ATRP) to synthesis narrowly distributed thiol-terminated 4-arm polystyrene star chains. Upon oxidation, we could slowly convert these chains in a semidilute solution to form branched polymer clusters through the formation of disulfide linkages ( $-S-S-$ ) between each two end thiol groups, as shown in Figure 1. Initially, it has only one expected peak related to individual star chains, but oxidation (cross-linking) results in a bimodal distribution. The second peak located at a longer relaxation time, confirming that thiol-terminated polystyrene star chains were cross-linked to form clusters in the solution. Static LLS has been used to characterize the structures of such formed clusters in a dilute solution. The inset shows that the average scattering intensity  $\langle I(q) \rangle$  of the resultant clusters is dependent on the scattering vector ( $q$ ) as  $\langle I(q) \rangle \propto q^{-d_f}$  with  $d_f = 2.6 \pm 0.1$ , indicating that the clustering is a RLCA process and results in compact aggregates. This is understandable because the cross-linking reaction in here was so slow that many collisions are required before the chains can stick together. Moreover, the extensive interchain penetration and cluster restructuring are expected to accompany the cross-linking reaction, allowing the clusters so formed to pack more closely and uniform. These behaviors have been observed in the studies of linear chains association<sup>2</sup> or aggregation of soft microgel particles.<sup>13</sup>

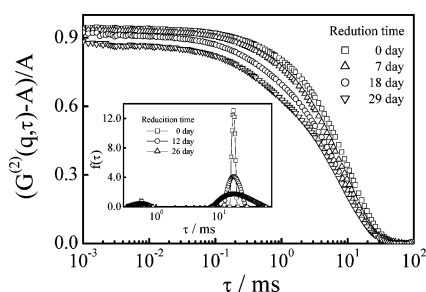
On the other hand, it is worth pointing out that the formed  $-S-S-$  linkages can be cleaved by reduction so that the formed clusters can undergo the decomposition (fragmentation). In this Communication, we like to report the structure and kinetics of cluster decomposition of such polystyrene star chains in a dilute solution. An analysis of light scattering data showed that the fragments could be characterized as a fractal, and both the structure and decomposition kinetics followed the reversible RLCA process. The thiol-terminated 4-arm polystyrene star chains preparation and LLS theory and instrumentation can be found elsewhere.<sup>16,17</sup>

Figure 2 shows that upon addition of 2,3-dihydroxy-1,4-butanethiol (DTT), a reducing agent, to a diluted cluster solution the slow relaxations became slight faster, but at the same time their contributions to the time average intensity–intensity correlation function  $[(G^{(2)}(q, \tau) - A)/A]$  decreased gradually as the reduction proceeded. Supposedly, this is contributed to the decrease of the number of larger clusters because some of them were decomposed into smaller fragments or even more mobile individual chains. We analyzed each measured  $[(G^{(2)}(q, \tau) - A)/A]$  by the Laplace inversion program (CONTIN) in the correlator to yield a normalized intensity-weighted distribution of the characteristic decay time  $f(\tau)$ . The inset in Figure 2 shows that for each measured  $(G^{(2)}(q, \tau) - A)/A$  at desired times during the decomposition process there always exists two relaxation modes. The fast mode is due to the diffusion of individual star chains, while the slow mode may be related to the mixture of fragments with different size. Both distributions of the characteristic decay time become broader and broader as the reduction

\* To whom correspondence should be addressed.



**Figure 1.** Peak area-normalized intensity distributions of characteristic decay time  $f(\tau)$  of thiol-terminated 4-arm polystyrene star chains before and after the cross-linking reaction, where  $\theta = 20^\circ$  and  $T = 25^\circ\text{C}$ . The inset shows a double-logarithmic plot of scattering intensity from resultant clusters  $\langle I(q) \rangle$  vs scattering vector  $q$  after the cross-linking reaction.



**Figure 2.** Reduction time dependence of the normalized intensity-intensity time correlation functions  $(G^{(2)}(q, \tau) - A)/A$  during the cluster decomposition process, where  $A$  is the measured baseline,  $\theta = 20^\circ$ , and  $T = 25^\circ\text{C}$ . The inset shows the time dependence of peak area-normalized intensity distributions of characteristic decay time  $f(\tau)$  at different times during the cluster decomposition.

proceeds, indicating that the solution becomes heterogeneous as individual chains, smaller and larger clusters coexist in the final mixture.

Here, we concentrated on the features of the fragments during the decomposition process; we therefore tried to quantitatively extract more information that only related to fragments but exclude the fast relaxation modes contributed in the  $(G^{(2)}(q, \tau) - A)/A$ . We assumed that the light scattering measured by both static and dynamic LLS is simply a sum over the average distribution of individual star chains and fragments. This is reasonable because from the dynamic LLS results, as shown in the inset of Figure 2, CONTIN analysis has only resulted in two characteristic, yet distinct, relaxation modes. Moreover, from the corresponding normalized areas under the two peaks, we could have the weight-average contribution from the fast ( $W(q)_{\text{chain}}$ ) and slow ( $W(q)_{\text{cluster}}$ ) modes. Note that  $W(q)_{\text{chain}} + W(q)_{\text{cluster}} = 1$ . Therefore, the time average scattering intensity contributed from the fragments can be obtained from total time average scattering intensity  $\langle I(q) \rangle_T$  measured in static LLS and  $W(q)_{\text{cluster}}$  from dynamic LLS, i.e.,  $\langle I(q) \rangle = \langle I(q) \rangle_T W(q)_{\text{cluster}}$ . In addition, by using the Ornstein-Zernike equation  $[I(q)] = [I(q \rightarrow 0)] / (1 + q^2 \langle \xi \rangle^2)$ ,<sup>18</sup> the plot of  $1/\langle I(q) \rangle$  vs  $q^2$  can lead to average correlation length of the fragments ( $\langle \xi \rangle$ ) and the time average scattering intensity at  $q \rightarrow 0$  ( $\langle I(0) \rangle$ ) (see the Supporting Information). It is helpful to mention that  $\langle I(0) \rangle$  is linearly to the weight-average molar mass ( $\langle M_w \rangle$ ) of the fragments during the decomposition process.

Figure 3a shows that the scattering intensity  $\langle I(q) \rangle$  of the fragments at different times during the fragmentation process is dependent on the scattering vector  $q$  as  $\langle I(q) \rangle \propto q^{-d_f}$  with all  $d_f$  in the range 2.2–2.6, indicating that the fragments are surprisingly characterized as a fractal. The slight decrease of  $d_f$  reveals that the fragments become relative more open and less

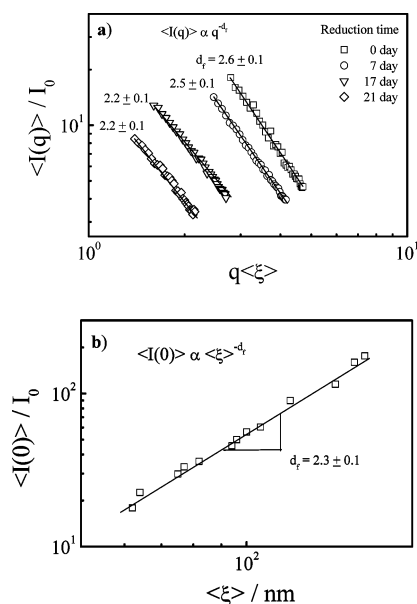


**Figure 3.** (a) Double-logarithmic plots of scattering intensity from resultant fragments  $\langle I(q) \rangle$  vs scattering vector  $q$  during the decomposition process. (b) Double-logarithmic plot of time-average scattering intensity at  $q \rightarrow 0$  ( $\langle I(0) \rangle$ ) vs average static correlation length scattering  $\langle \xi \rangle$  for resultant fragments formed at different times during the decomposition process.

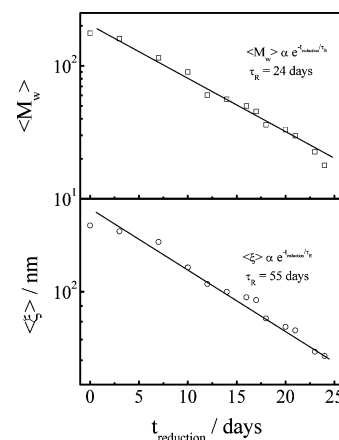


**Figure 4.**  $\langle M_w \rangle$  and  $\langle \xi \rangle$  as a function of decomposition time. Both the scales of  $\langle M_w \rangle$  and  $\langle \xi \rangle$  are logarithmic to show the exponential decay.

uniform because the  $-S-S-$  linkages inside the clusters are cleaved. To best of our knowledge, this is the first example to show the structure of fragments during the decomposition process, particularly for those clusters formed by covalent bonds. It is helpful to mention that the data were all collected when  $q\langle \xi \rangle > 1$ , and all  $d_f > 2$  suggests that the decomposition process is the RLCA process. Unfortunately, since the sizes of the fragments are not big enough, the range of  $q$  presented in here can only spread over limited ranges. Figure 3b shows that at different times during the decomposition process  $\langle I(0) \rangle$  is scaled to  $\langle \xi \rangle$  as  $\langle I(0) \rangle \propto \langle \xi \rangle^{-d_f}$  or  $\langle M_w \rangle \propto \langle \xi \rangle^{-d_f}$ , with  $d_f = 2.3 \pm 0.1$ , an alternative way to reveal that it is a RLCA process.

Since both  $\langle M_w \rangle$  and  $\langle \xi \rangle$  can accurately reflect the weight-average molar mass and size of fragments in the distribution at each time during the decomposition process, they are two important parameters to measure the decomposition kinetics. Figure 4 shows that both  $\langle M_w \rangle$  and  $\langle \xi \rangle$  exponentially decrease during the decomposition, namely,  $\langle M_w \rangle \propto e^{-t/t_R}$  and  $\langle \xi \rangle \propto e^{-t/t_R}$  with  $t_R = 24$  and 55 days, respectively. Note that RLCA has a typically exponential growth in kinetics; the results presented

here thereby provide another evidence that decomposition is a reversible RLCA process.

In summary, using narrowly distributed thiol-terminated 4-arm polystyrene star chains enabled us to controllably and reversibly study the formation and decomposition of branched polystyrene clusters. As expected, the clustering is a reaction-limited process, and the resultant clusters have a fractal structure with a fractal dimension of  $2.6 \pm 0.1$ . Surprisingly, our results show that the fragments formed during the decomposition are also fractals with a fractal dimension ( $d_f$ ) of 2.2–2.6; namely, their time-average scattering intensity ( $I(q)$ ) is scalable to the scattering vector ( $q$ ) as  $\langle I(q) \rangle \propto \langle q \rangle^{-d_f}$ , and the weight-average molar mass ( $M_w$ ) of the fragments is scalable to the average size of the fragments ( $\langle \xi \rangle$ ) as  $\langle M_w \rangle \propto \langle \xi \rangle^{2.3 \pm 0.1}$ . Both  $\langle M_w \rangle$  and  $\langle \xi \rangle$  exponentially decrease during the decomposition, revealing that it is also a reaction-limited process. Previously, we only know that some of the clustering process is reaction-limited. This study enables us to realize that both formation and decomposition (fragmentation) of hyperbranched polystyrene clusters with –S–S– linkages follow the reaction-limited mechanism.

**Acknowledgment.** We thank Prof. Chi Wu (Department of Chemistry, The Chinese University of Hong Kong) for the helpful discussions. The financial support of this work by the Hong Kong Special Administration Region (HKSAR) Earmarked Project (CUHK402506, 2160291), the Direct Grant for Research 2006/07 of the Chinese University of Hong Kong (CUHK 2060303), and a key research grant (20534020) from the National Natural Scientific Foundation of China (NNSFC) is gratefully acknowledged.

**Supporting Information Available:** Typical Ornstein–Zernike plots of  $1/\langle I(q) \rangle$  vs  $q^2$ . This material is available free of charge via the Internet at <http://pubs.acs.org>.

## References and Notes

- (1) Takeda, M.; Norisuye, T.; Shibayama, M. *Macromolecules* **2000**, *33*, 2909.
- (2) Peng, S. F.; Wu, C. *Macromolecules* **2001**, *34*, 6795.
- (3) Richter, S.; Boyko, V.; Schröter, K. *Macromol. Rapid Commun.* **2004**, *25*, 542.
- (4) Weitz, A. D.; Lin, M. Y.; Huang, J. S. *Physics of Complex and Supermolecular Fluids*; Wiley-Interscience: New York, 1987.
- (5) Weitz, A. D.; Huang, J. S.; Lin, M. Y.; Sung, J. *Phys. Rev. Lett.* **1985**, *54*, 1416.
- (6) Lin, M. Y.; Lindsay, H. M.; Weitz, A. D.; Ball, R. C.; Klein, R.; Meakin, P. *Nature (London)* **1989**, *339*, 360.
- (7) Russel, W. B.; Saville, D. A.; Schowalter, W. R. *Colloidal Dispersions*; Cambridge University Press: New York, 1989.
- (8) Lin, M. Y.; Lindsay, H. M.; Weitz, A. D.; Ball, R. C.; Klein, R.; Meakin, P. *J. Phys.: Condens. Matter* **1990**, *2*, 3093.
- (9) Lin, M. Y.; Lindsay, H. M.; Weitz, A. D.; Ball, R. C.; Klein, R.; Meakin, P. *Phys. Rev. A* **1990**, *41*, 2005.
- (10) Zhou, Z.; Wu, P.; Chu, B. *J. Colloid Interface Sci.* **1991**, *146*, 541.
- (11) Asnaghi, D.; Carpineti, M.; Giglio, M.; Sozzi, M. *Phys. Rev. A* **1992**, *45*, 1018.
- (12) Dimon, P.; Sinha, S. K.; Weitz, D. A.; Safinya, C. R.; Smith, G. S.; Varady, W. A.; Lindsay, H. M. *Phys. Rev. Lett.* **1986**, *57*, 595.
- (13) Zhu, P. W.; Napper, D. H. *Phys. Rev. E* **1994**, *50*, 1360.
- (14) Fernandez-Nieves, A.; Fernandez-Barbero, A.; Vincent, B.; de las Nieves, F. J. *Langmuir* **2001**, *17*, 1841.
- (15) Niu, A.-Z.; Li, C. M.; Zhao, Y.; He, J. P.; Yang, Y. L.; Wu, C. *Macromolecules* **2001**, *34*, 460.
- (16) Aliyar, H. A.; Hamilton, P. D.; Ravi, N. *Biomacromolecules* **2005**, *6*, 204.
- (17) Chu, B. *Laser Light Scattering*, 2nd ed.; Academic: New York, 1991.
- (18) Soni, V. K.; Stein, R. S. *Macromolecules* **1990**, *23*, 5257.

MA071299+